

Equivalent retarder approach to reflective liquid crystal displays

S. Stallinga^{a)}

Philips Research Laboratories, Professor Holstlaan 4, 5656 AA Eindhoven, The Netherlands

(Received 19 April 1999; accepted for publication 7 August 1999)

Reflective liquid crystal displays (LCDs) are studied using the Jones 2×2 matrix method. The reflective LCD effectively behaves as a single retardation layer. Conditions on the retardation and optical axis orientation of this equivalent retarder in order to obtain high brightness and high contrast are derived and applied to twisted nematic layers without and with a compensating waveplate. The optimization of the display performance by numerical calculations is greatly simplified by analytical results relating the parameters of the liquid crystal, incident polarization, and compensator. © 1999 American Institute of Physics. [S0021-8979(99)08921-5]

I. INTRODUCTION

Reflective liquid crystal displays (LCDs) are interesting from the point of view of two different applications. The absence of a backlight makes them suitable for portable electronic equipment with little energy consumption. Alternatively, combined with monocrystalline active matrix arrays they can be applied in compact high resolution projectors. Optimizing the performance of these displays requires understanding of the propagation of polarized light through a reflective LCD. In a recent article¹ I have described the use of the Berreman 4×4 matrix method for reflective LCDs. This method is basic to most numerical calculations of the optical properties of LCDs. This article deals with the Jones 2×2 matrix method. In this method only the primary reflection at the mirror is taken into account, as opposed to the Berreman method, in which all reflections at all interfaces are taken into account. Within the framework of the Jones method many analytical results can be derived. It is the goal of this article to use such results to simplify and speed up numerical optimization and aid the physical understanding of the optics of reflective LCDs.

The main result presented in this article is that any set of birefringent layers in front of a mirror behaves effectively as a single retardation layer. Clearly, the retardation and optical axis angle of this fictitious equivalent retarder are then sufficient to characterize the system. On the basis of this result conditions for minimum and maximum reflection can be easily formulated. These conditions can be used for calculating the liquid crystal parameter values that give rise to optimum brightness and contrast of reflective LCDs.

The content of this article is as follows. In Sec. II expressions for the Jones matrices relevant to reflective systems are presented and the equivalent retarder approach is introduced. This approach is used to formulate requirements for optimum brightness and contrast. These requirements are applied to twisted nematics without a compensating waveplate in Sec. III and to twisted nematics with a compensating waveplate in Sec. IV. The article is concluded in Sec. V with a summary of the main conclusions.

II. EQUIVALENT RETARDER APPROACH

The Jones 2×2 matrix method deals with light propagating along the normal of a stack of planparallel uniform layers. Taking the z axis along the normal the x and y components of the electric field E_x and E_y at the exit side of the stack are linearly dependent on E_x and E_y at the entry side, and the proportionality coefficients are the components of the Jones matrix \mathcal{J} ²

$$\begin{bmatrix} E_x \\ E_y \end{bmatrix}_{\text{out}} = \begin{bmatrix} J_{11} & J_{12} \\ J_{21} & J_{22} \end{bmatrix} \begin{bmatrix} E_x \\ E_y \end{bmatrix}_{\text{in}} \equiv \mathcal{J} \begin{bmatrix} E_x \\ E_y \end{bmatrix}_{\text{in}}. \quad (1)$$

The Jones matrix for light propagating backwardly, i.e., from the “out-side” to the “in-side” is also \mathcal{J} , provided that the electric field components are written as a row vector instead of as a column vector.² When the electric field is written as a column vector the Jones matrix for light propagating backwardly is \mathcal{J}^T , the transpose of \mathcal{J}

$$\begin{bmatrix} E'_x \\ E'_y \end{bmatrix}_{\text{in}} = \begin{bmatrix} J_{11} & J_{21} \\ J_{12} & J_{22} \end{bmatrix} \begin{bmatrix} E'_x \\ E'_y \end{bmatrix}_{\text{out}} \equiv \mathcal{J}^T \begin{bmatrix} E'_x \\ E'_y \end{bmatrix}_{\text{out}}, \quad (2)$$

where the accent indicates light propagating backwardly. A proof based on the Berreman 4×4 matrix method can be found in the Appendix. It is remarked that the same coordinate frame is used to describe light propagating in the two directions. As a consequence, one and the same Jones vector describes polarization states with a different handedness for the two directions of propagation.

Consider the case where an ideal mirror is placed on one side of the stack. The backwardly propagating field at the mirror depends on the incident field as

$$\begin{bmatrix} E'_x \\ E'_y \end{bmatrix}_{\text{mirror}} = \mathcal{J}^T \begin{bmatrix} E_x \\ E_y \end{bmatrix}_{\text{in}}, \quad (3a)$$

whereas the reflected field depends on the forwardly propagating field at the mirror by

$$\begin{bmatrix} E_x \\ E_y \end{bmatrix}_{\text{out}} = \mathcal{J} \begin{bmatrix} E_x \\ E_y \end{bmatrix}_{\text{mirror}}. \quad (3b)$$

The forwardly and backwardly propagating fields at the mirror are related by the phase jump equal to π , leading to

^{a)}Electronic mail: sjoero.stallinga@philips.com

$$\begin{bmatrix} E_x \\ E_y \end{bmatrix}_{\text{mirror}} = - \begin{bmatrix} E'_x \\ E'_y \end{bmatrix}_{\text{mirror}}. \quad (3c)$$

This overall minus sign may be ignored. Combining these three equations gives the relation between the reflected and incident fields as

$$\begin{bmatrix} E_x \\ E_y \end{bmatrix}_{\text{out}} = \mathcal{J}_r \begin{bmatrix} E_x \\ E_y \end{bmatrix}_{\text{in}}, \quad (4)$$

where the Jones matrix for reflection is equal to the product of \mathcal{J} and its transpose

$$\mathcal{J}_r = \mathcal{J} \mathcal{J}^T. \quad (5)$$

It follows that \mathcal{J}_r is a symmetric matrix, because:

$$\mathcal{J}_r^T = (\mathcal{J} \mathcal{J}^T)^T = \mathcal{J} \mathcal{J}^T = \mathcal{J}_r. \quad (6)$$

The same result has appeared in Ref. 3. It is noted that the same reference frame is used before and after reflection.

$$\mathcal{J} = \begin{bmatrix} \cos \delta \cos \theta + i \sin \delta \cos(\theta + 2\gamma) & -\cos \delta \sin \theta + i \sin \delta \sin(\theta + 2\gamma) \\ \cos \delta \sin \theta + i \sin \delta \sin(\theta + 2\gamma) & \cos \delta \cos \theta + i \sin \delta \cos(\theta + 2\gamma) \end{bmatrix}. \quad (7d)$$

Equations (7) mean that any birefringent system may be replaced by an effective retarder and an effective rotator. This effective retarder introduces a phase difference 2δ between two eigenwaves that are linearly polarized at angles γ and $\gamma + \pi/2$ with the x axis, whereas the effective rotator rotates the polarization ellipse over an angle θ . Clearly, the action of an arbitrary birefringent system on polarized light can be described by the three parameters γ , δ , and θ .

For a birefringent stack with an ideal mirror placed at the bottom of the stack, the Jones matrix for reflection takes a special form. Given that the Jones matrix for forward propagation can be expressed according to Eqs. (7), the Jones matrix for backward propagation can then be written as

$$\mathcal{J}^T = \mathcal{R}(-\theta) \mathcal{R}(\gamma) \mathcal{U}(g\delta) \mathcal{R}(-\gamma), \quad (8)$$

and the Jones matrix for reflection as

$$\mathcal{J}_r = \mathcal{J} \mathcal{J}^T = \mathcal{R}(\gamma) \mathcal{U}(2\delta) \mathcal{R}(-\gamma). \quad (9)$$

Apparently, the effective rotator components cancel each other, while the effective retarder components add up. This means that the action of a reflective birefringent system on polarized light is equivalent to that of a single retardation layer, described by two parameters γ and δ . This is shown schematically in Fig. 1. The physical symmetry underlying this result is the invariance under time reversal of Maxwell's equations. This symmetry specifies the electromagnetic field when the direction of propagation is reversed. Time reversal invariance leads to the same result in the framework of the exact Berreman 4×4 matrix method.¹

Suppose that the birefringent layers are sandwiched between an ideal mirror at the bottom and an ideal polarizer on top. This describes a direct view reflective LCD. When the transmission axis of the polarizer makes an angle ψ with the

When the propagation direction is taken along the positive z direction a different coordinate frame is needed after reflection. As a consequence an additional matrix enters the expression for \mathcal{J}_r . In the absence of absorption Jones matrices are unitary matrices, the determinant of which can be taken equal to one. Such a matrix \mathcal{J} can always be expressed in the following form:⁴

$$\mathcal{J} = \mathcal{R}(\gamma) \mathcal{U}(\delta) \mathcal{R}(-\gamma) \mathcal{R}(\theta), \quad (7a)$$

with the retardation matrix

$$\mathcal{U}(\delta) = \begin{bmatrix} \exp(i\delta) & 0 \\ 0 & \exp(-i\delta) \end{bmatrix}, \quad (7b)$$

and the rotation matrix

$$\mathcal{R}(\phi) = \begin{bmatrix} \cos \phi & -\sin \phi \\ \sin \phi & \cos \phi \end{bmatrix}. \quad (7c)$$

This leads to the explicit expression:

x axis, the requirements for a reflection coefficient equal to one or equal to zero can now be easily formulated in terms of the parameters γ and δ of the equivalent retarder. The reflection coefficient equals zero if (and only if) the equivalent retarder is a $\lambda/2$ plate with its optical axis at $\pi/4$ with the polarizer axis, i.e.,

$$2\delta = \pi/2, \quad (10a)$$

and

$$\gamma = \psi \pm \pi/4. \quad (10b)$$

The reflection coefficient equals unity if either the effective retardation equals zero or if the effective optical axis is aligned with the polarizer transmission or absorption axis, i.e.,

$$2\delta = 0, \quad (11a)$$

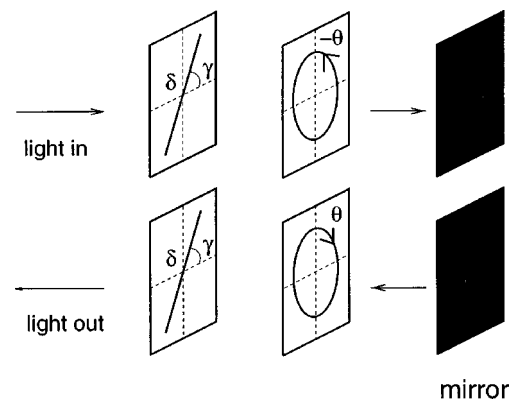


FIG. 1. The polarization rotation for backward propagation cancels that for forward propagation leaving only retardation.

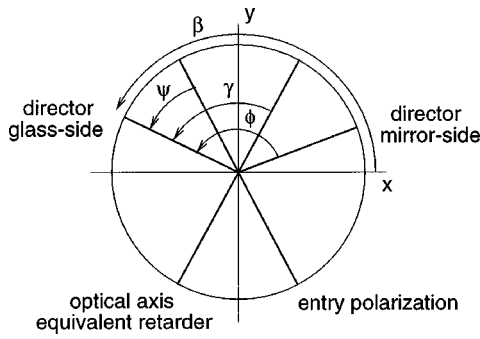


FIG. 2. The relative orientation of the director on the top/glass side, the director on the bottom/mirror side of the cell, the equivalent retarder optical axis, and the polarization of the light incident on the display.

or

$$\gamma = \begin{cases} \psi, \\ \psi + \pi/2. \end{cases} \quad (11b)$$

It is remarked that these conditions can also be derived from the rather simple expression for the reflection coefficient in terms of ψ , γ , and δ

$$R = 1 - \sin^2(2\delta)\sin^2(2\gamma - 2\psi). \quad (12)$$

Equations (10) and (11) are applied to the twisted nematic effect in the next two sections.

For a direct view reflective LCD the polarizer is also the analyzer, i.e., the incident and selected polarization are the same. This is different from a reflective LCD in a projector, which is illuminated through a polarizing beam splitter (PBS). A PBS transmits light of one polarization and reflects light of the orthogonal polarization. The reflective LCD is placed in the beam reflected by the PBS. The beam is incident on the PBS for the second time after being reflected at the LCD. Only if the reflective LCD changes the polarization is the beam transmitted by the PBS, and projected on the screen. It follows that the selected polarization is orthogonal to the incident polarization. The reflective LCD/PBS combination can thus be seen as a reflective LCD “between” crossed polarizers, whereas the direct view variant can be seen as a reflective LCD between parallel polarizers. As a consequence, the reflection coefficient R of direct view displays must be replaced by $1 - R$ for projection displays, the conditions for zero reflection are now the conditions for unity reflection, whereas the conditions for unity reflection are now the conditions for zero reflection.

III. TWISTED NEMATIC LIQUID CRYSTAL EFFECT

Consider a twisted nematic liquid crystal layer of twist angle ϕ (which is positive if the twist is right handed), thickness d , and birefringence Δn . The director makes an angle β with the x axis on the top side (at $z=d$), and $\beta - \phi$ at the bottom side (at $z=0$), as shown in Fig. 2. In order to analyze brightness and contrast expressions for the Jones matrix in the addressed and nonaddressed states are required. In a first approximation the director profile in the addressed state may be considered homeotropic so that there is no retardation left. The Jones matrix is then the unity matrix. Consequently, the

driven state is the bright state for direct view type reflective LCDs, whereas it is the dark state for projection type reflective LCDs, with ideal reflection coefficients $R=1$ and $R=0$, respectively. This means that direct view displays are normally black, whereas projection displays are normally white. The nonaddressed state may be approximated as a nontilted uniformly twisted layer, provided that the surface pretilt is sufficiently small. The Jones matrix (for forward propagation) can then be expressed as⁵⁻⁷

$$J = R(\beta)KR(-\beta + \phi), \quad (13)$$

where K is the Jones matrix in the frame that corotates with the twisting director, and is given by

$$K = \begin{bmatrix} \cos(\pi\Gamma) + i\frac{v}{\Gamma}\sin(\pi\Gamma) & \frac{u}{\Gamma}\sin(\pi\Gamma) \\ -\frac{u}{\Gamma}\sin(\pi\Gamma) & \cos(\pi\Gamma) - i\frac{v}{\Gamma}\sin(\pi\Gamma) \end{bmatrix}. \quad (14)$$

The quantities u , v , and Γ are defined as

$$u = \frac{\phi}{\pi}, \quad (15a)$$

$$v = \frac{d\Delta n}{\lambda}, \quad (15b)$$

$$\Gamma = \sqrt{u^2 + v^2}. \quad (15c)$$

The Jones matrix of the twisted nematic layer can also be expressed in terms of an effective retarder with retardation δ and optical axis at an angle $\beta - \gamma$ with the x axis (which means an angle γ with the director on the top side) and an effective rotator over θ as

$$J = R(\beta - \gamma)U(\delta)R(-\beta + \gamma)R(\theta). \quad (16)$$

Consequently

$$K = R(-\gamma)U(\delta)R(\theta + \gamma - \phi) \\ = \begin{bmatrix} \cos \delta \cos(\theta - \phi) & -\cos \delta \sin(\theta - \phi) \\ +i \sin \delta \cos(2\gamma - \phi + \theta) & +i \sin \delta \sin(2\gamma - \phi + \theta) \\ \cos \delta \sin(\theta - \phi) & \cos \delta \cos(\theta - \phi) \\ +i \sin \delta \sin(2\gamma - \phi + \theta) & -i \sin \delta \cos(2\gamma - \phi + \theta) \end{bmatrix}. \quad (17)$$

It follows directly that

$$\theta = \phi - 2\gamma. \quad (18)$$

This relation is a consequence of the symmetry of the director profile.⁷ The layer does not change when rotated over π around an axis perpendicular to the plane spanned by the layer normal and the director at $z=d/2$ (midplane director). This symmetry is also present for driven LCDs, from which it follows that Eq. (18) also holds when a voltage is applied. Using Eq. (18), the relations between γ and δ on one side, and ϕ/π and $d\Delta n/\lambda$ on the other now follow as

$$\cos \delta \cos(2\gamma) = \cos(\pi\Gamma), \quad (19a)$$

$$\sin \delta = \frac{v}{\Gamma} \sin(\pi\Gamma), \quad (19b)$$

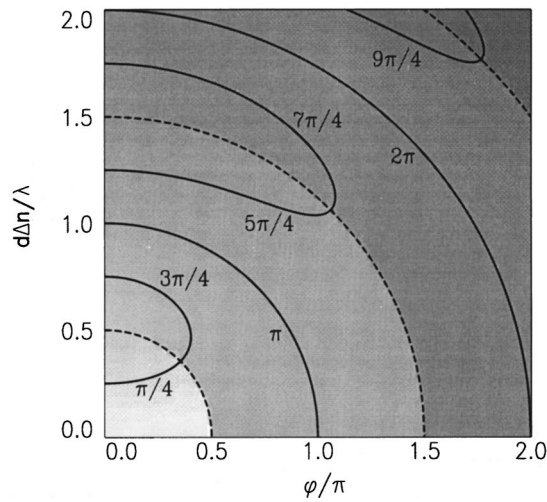


FIG. 3. Contour plot of δ in the uv plane. The δ values range from 0 (light gray) to approximately 3π (dark gray). The full lines are contours of fixed δ , the dashed lines are the singular lines or branch cuts.

$$\cos \delta \sin(2\gamma) = \frac{u}{\Gamma} \sin(\pi\Gamma). \quad (19c)$$

Equations (19) can be solved for γ and δ or for ϕ/π and $d\Delta n/\lambda$. In the first case δ follows from Eq. (19b) and γ from Eqs. (19a) and (19c). It is found that

$$\delta = m\pi + (-1)^m \arcsin\left\{\frac{v}{\Gamma} \sin(\pi\Gamma)\right\}, \quad (20a)$$

$$2\gamma = m\pi + \arctan\left\{\frac{u}{\Gamma} \tan(\pi\Gamma)\right\}, \quad (20b)$$

where m is an integer, the choice of which is arbitrary. For any choice of m singularities appear in the uv plane, meaning that points and/or lines are not characterized by a unique pair of δ and γ values. If it is required that δ and γ are nonsingular along the $v = d\Delta n/\lambda$ axis and $u = \phi/\pi$ axis, then m must be the largest integer smaller than $\Gamma - 1/2$ ($m=0$ if $0 \leq \Gamma < 1/2$, $m=1$ is $1/2 \leq \Gamma < 3/2$, etc.). Figures 3 and 4 show contour plots for this choice of m of δ and γ , respectively.

We now turn to the second case, solving u and v in terms of γ and δ . First, Γ follows from Eq. (19a) as

$$\Gamma = \frac{2k+1}{2} - (-1)^k \frac{\arcsin\{\cos \delta \cos(2\gamma)\}}{\pi}, \quad (21)$$

with k an integer. It then follows that

$$\sin(\pi\Gamma) = (-1)^k \sqrt{\sin^2 \delta + \cos^2 \delta \sin^2(2\gamma)}. \quad (22)$$

Using Eqs. (19b) and (19c) ϕ/π and $d\Delta n/\lambda$ can now be expressed as

$$\begin{aligned} \frac{\phi}{\pi} &= (-1)^k \frac{\cos \delta \sin(2\gamma)}{\sqrt{\sin^2 \delta + \cos^2 \delta \sin^2(2\gamma)}} \\ &\times \left[\frac{2k+1}{2} - (-1)^k \frac{\arcsin\{\cos \delta \cos(2\gamma)\}}{\pi} \right], \end{aligned} \quad (23a)$$

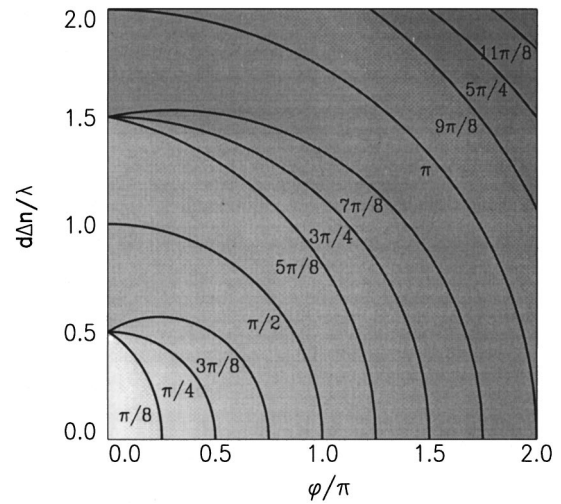


FIG. 4. Contour plot of γ in the uv plane. The γ values range from 0 (light gray) to approximately $3\pi/2$ (dark gray). The full lines are contours of fixed γ . There are singular points on the v axis (at $v=1/2, 3/2, 5/2, \dots$).

$$\begin{aligned} \frac{d\Delta n}{\lambda} &= (-1)^k \frac{\sin \delta}{\sqrt{\sin^2 \delta + \cos^2 \delta \sin^2(2\gamma)}} \\ &\times \left[\frac{2k+1}{2} - (-1)^k \frac{\arcsin\{\cos \delta \cos(2\gamma)\}}{\pi} \right]. \end{aligned} \quad (23b)$$

Just as before, the choice of the integer k is arbitrary. It turns out that each branch k gives values for u and v such that $k \leq \Gamma < k+1$. Figures 5 and 6 show $u = \phi/\pi$ and $v = d\Delta n/\lambda$ as a function of δ and γ for $k=0$. Clearly, u and v are invariant under the combined substitution $\delta \rightarrow \delta + \pi$ and $\gamma \rightarrow \gamma + \pi/2$.

Using Eqs. (23) and the conditions for zero or unity reflection analytical expressions are found for the twist angle and retardance in terms of the angle ψ between the entry

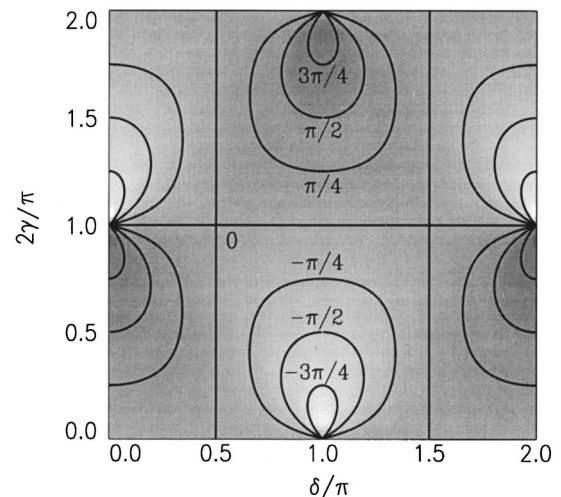


FIG. 5. Contour plot of ϕ in the $\delta\gamma$ plane for the branch $k=0$. The ϕ values range from $-\pi$ (light gray) to π (dark gray). The full lines are contours of fixed ϕ . Singular points are located on a square grid with integer coordinates (l, m) such that $l+m$ is odd.

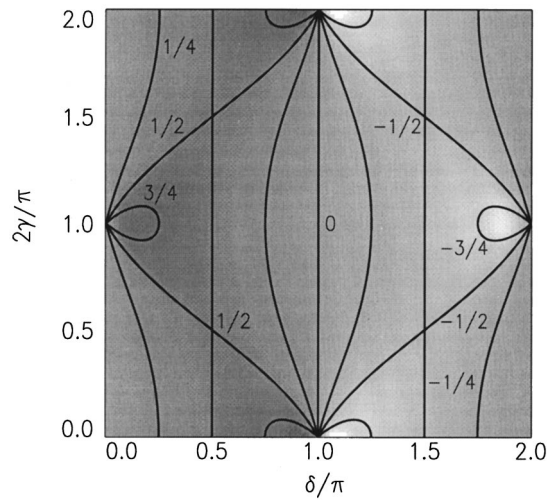


FIG. 6. Contour plot of $d\Delta n/\lambda$ in the $\delta\gamma$ plane for the branch $k=0$. The $d\Delta n/\lambda$ values range from -1 (light gray) to 1 (dark gray). The full lines are contours of fixed $d\Delta n/\lambda$. Singular points are located on a square grid with integer coordinates (l, m) such that $l+m$ is odd.

polarization and the top side director. This polarization makes an angle $\beta - \psi$ with the x axis, as shown in Fig. 2.

The bright state conditions for a (normally white) projection type display follow from combining Eqs. (10) and (23):

$$\frac{\phi}{\pi} = (-1)^k \frac{\cos(2\psi)}{\sqrt{1 + \cos^2(2\psi)}} \times \left[\frac{2k+1}{2} + (-1)^k \frac{\arcsin\{\sin(2\psi)/\sqrt{2}\}}{\pi} \right], \quad (24a)$$

$$\frac{d\Delta n}{\lambda} = (-1)^k \frac{1}{\sqrt{1 + \cos^2(2\psi)}} \times \left[\frac{2k+1}{2} + (-1)^k \frac{\arcsin\{\sin(2\psi)/\sqrt{2}\}}{\pi} \right]. \quad (24b)$$

It is proposed here to adopt the shorthand $\phi\text{TN}\psi$ for “the twisted nematic effect with twist angle ϕ and a linear entry polarization at an angle ψ with the director on the entry side of the liquid crystal.” The most well-known effect is then termed as the 63TN0 effect, which has $k=0$ and $\psi=0$, and hence $\phi = \sqrt{2}\pi/4 = 63.6^\circ$ and $d\Delta n/\lambda = \sqrt{2}/4 = 0.354$.⁸⁻¹¹ Another case is the “self-compensating” 60TN30 effect, invented by H. A. van Sprang¹² and later rediscovered.¹³ This effect has $\psi = \phi/2$, i.e., the entry polarization is parallel to the midcell director. As a consequence, the twist angle satisfies

$$\frac{\phi}{\pi} = (-1)^k \frac{\cos \phi}{\sqrt{1 + \cos^2 \phi}} \times \left[\frac{2k+1}{2} + (-1)^k \frac{\arcsin\{\sin \phi/\sqrt{2}\}}{\pi} \right], \quad (25)$$

which for $k=0$ gives $\phi = 58.67^\circ$ and $d\Delta n/\lambda = 0.627$. The limiting case of the nontwisted electrically controlled birefringence effect is described by the cases $\psi = \pm \pi/4$. Within

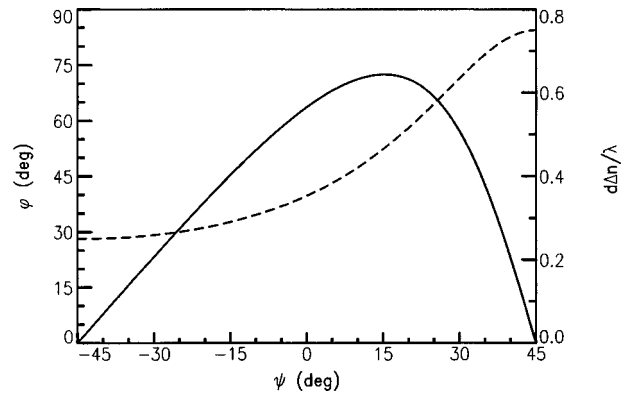


FIG. 7. The values of ϕ (full line, left y axis) and $d\Delta n/\lambda$ (dashed line, right y axis) of the branch $k=0$ giving rise to optimum brightness of a normally white projection reflective LCD without compensator as a function of the polarizer angle ψ .

the present nomenclature they would be termed as 0TN-45 and 0TN45. The branch in the $d\Delta n/\lambda - \phi/\pi$ plane with index k coincides with the contour lines $\delta = (4k + 2 \pm 1)\pi/4$ in Fig. 3. Figures 7 and 8 show the relation between $d\Delta n/\lambda$, ϕ , and ψ for the branch $k=0$. Remarkably, the twist angle is restricted to values smaller than approximately 72° . The branches with $k \geq 1$ have higher twist angles. The relation between $d\Delta n/\lambda$ and ϕ has been derived before in Ref. 11, but not in the explicit form of Eqs. (24).

The bright state conditions for a (normally black) direct view type display follow from combining Eqs. (11) and (23)

$$\frac{\phi}{\pi} = (-1)^k \frac{\cos \delta \sin(2\psi)}{\sqrt{\sin^2 \delta + \cos^2 \delta \sin^2(2\psi)}} \times \left[\frac{2k+1}{2} - (-1)^k \frac{\arcsin\{\cos \delta \cos(2\psi)\}}{\pi} \right], \quad (26a)$$

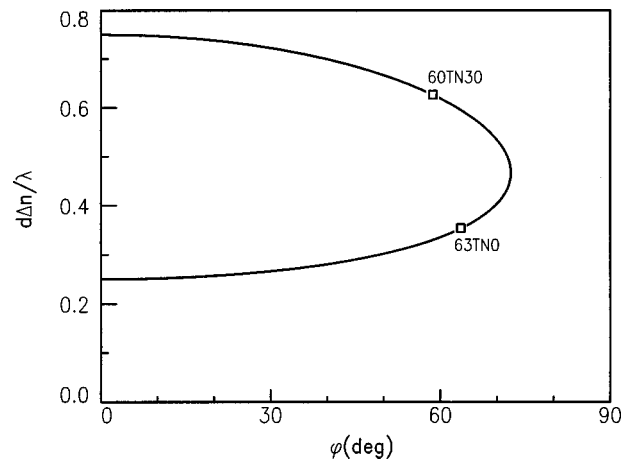


FIG. 8. The ratio $d\Delta n/\lambda$ as a function of ϕ of the branch $k=0$ giving rise to optimum brightness of a normally white projection reflective LCD without compensator.

$$\frac{d\Delta n}{\lambda} = (-1)^k \frac{\sin \delta}{\sqrt{\sin^2 \delta + \cos^2 \delta \sin^2(2\psi)}} \times \left[\frac{2k+1}{2} - (-1)^k \frac{\arcsin\{\cos \delta \cos(2\psi)\}}{\pi} \right]. \quad (26b)$$

Here, δ is a free parameter. Clearly, any pair of values for ϕ and $d\Delta n/\lambda$ can give rise to a good dark state. The curves $\Gamma = k\pi$ with k an integer are the solutions already found in Ref. 14.

IV. TWISTED NEMATIC LIQUID CRYSTAL EFFECT WITH RETARDER

It turns out that quite high voltages are needed to achieve an addressed state which is practically isotropic. Drivers that can supply such high voltages are relatively expensive, and are therefore not used in practice. It then follows that in practical circumstances the addressed state always has a residual retardance. Clearly, the approximation used in the previous section does not hold in practice, meaning that a more refined treatment is needed. This treatment is based on numerical calculations, as no analytical expression for the Jones matrix in the addressed state are known.

The effect of a compensating retardation layer added to the display can be quite beneficial.^{14–18} Including a retarder makes the calculations even more complicated due to the increased number of degrees of freedom. Despite these dif-

ficulties, the requirements for a good bright and dark state Eqs. (10) and (11) in terms of the equivalent retarder parameters are still the same, and these conditions may be used to simplify the task of finding an optimum display configuration using numerical calculations. It is assumed that the compensator is placed on top of the liquid crystal layer and not in between the mirror and the liquid crystal. The latter case excludes the use of an in-cell reflector, which is needed to avoid parallax. It is remarked that the compensated driven state can have an arbitrary retardation, as opposed to the uncompensated driven state which has a limited retardation. This implies that the driven state can be the state which effectively behaves as a $\lambda/2$ plate, i.e., as a dark state for a direct view display and as a bright state for a projection display. Consequently, both the direct view as the projection type of reflective LCD can be normally white or normally black, provided that the liquid crystal is compensated by a retarder.

Starting point of the analysis are expressions for the Jones matrices of the liquid crystal and of the compensator. In these expressions the frame of reference is rotated around the z axis over an angle ψ , so that the new x axis is along the entry polarization. The Jones matrices of the liquid crystal in the two states A and B for reflection can then be expressed in terms of the effective waveplate parameters retardation values δ_A and δ_B and optical axis angles γ_A and γ_B at voltages V_A and V_B as

$$\mathcal{J}_A = \begin{bmatrix} \cos(2\delta_A) + i \sin(2\delta_A) \cos(2\gamma_A - 2\psi) & i \sin(2\delta_A) \sin(2\gamma_A - 2\psi) \\ i \sin(2\delta_A) \sin(2\gamma_A - 2\psi) & \cos(2\delta_A) - i \sin(2\delta_A) \cos(2\gamma_A - 2\psi) \end{bmatrix}, \quad (27a)$$

$$\mathcal{J}_B = \begin{bmatrix} \cos(2\delta_B) + i \sin(2\delta_B) \cos(2\gamma_B - 2\psi) & i \sin(2\delta_B) \sin(2\gamma_B - 2\psi) \\ i \sin(2\delta_B) \sin(2\gamma_B - 2\psi) & \cos(2\delta_B) - i \sin(2\delta_B) \cos(2\gamma_B - 2\psi) \end{bmatrix}. \quad (27b)$$

The effective waveplate parameters δ_A , δ_B , γ_A , and γ_B are calculated numerically from the director profile at V_A and V_B . If V_A or V_B are below threshold the analytical expressions for the retardation and optical axis angle derived in the previous section may be used without introducing a significant error. The compensator Jones matrix for transmission is

$$\mathcal{J}_R = \begin{bmatrix} \cos \delta_R + i \sin \delta_R \cos(2\gamma_R - 2\psi) & i \sin \delta_R \sin(2\gamma_R - 2\psi) \\ i \sin \delta_R \sin(2\gamma_R - 2\psi) & \cos \delta_R - i \sin \delta_R \cos(2\gamma_R - 2\psi) \end{bmatrix}. \quad (28)$$

According to Eqs. (10) and (11) the compensated state A is equivalent to a $\lambda/2$ plate with optical axis at $\pi/4$ with the entry polarization whereas the compensated state B is equivalent to a waveplate with retardation 2δ and optical axis parallel to the entry polarization. This means that state A is the dark state for direct view displays and the bright state for projection displays, whereas B is the bright state for direct view displays and the dark state for projection displays. Consequently, the overall Jones matrices for reflection of the liquid crystal/waveplate combination for state A and B are

$$\mathcal{J}_R \mathcal{J}_A \mathcal{J}_R = \mathcal{R}(\pi/4) \mathcal{U}(\pi/2) \mathcal{R}(-\pi/4) = \begin{bmatrix} 0 & i \\ i & 0 \end{bmatrix}, \quad (29a)$$

$$\mathcal{J}_R \mathcal{J}_B \mathcal{J}_R = \mathcal{U}(\delta) = \begin{bmatrix} \exp(i\delta) & 0 \\ 0 & \exp(-i\delta) \end{bmatrix}, \quad (29b)$$

or

$$\mathcal{J} = \mathcal{J}_R^{-1} \begin{bmatrix} 0 & i \\ i & 0 \end{bmatrix} \mathcal{J}_R^{-1}, \quad (30a)$$

$$\mathcal{J}_B = \mathcal{J}_R^{-1} \begin{bmatrix} \exp(i\delta) & 0 \\ 0 & \exp(-i\delta) \end{bmatrix} \mathcal{J}_R^{-1}, \quad (30b)$$

where \mathcal{J}_R^{-1} is found from the expression for \mathcal{J}_R by replacing δ_R by $-\delta_R$. After straightforward but lengthy matrix multiplication the following six expressions for the matrix elements of \mathcal{J}_A and \mathcal{J}_B are found

$$\cos(2\delta_A) = \sin(2\delta_R) \sin(2\gamma_R - 2\psi), \quad (31a)$$

$$\sin(2\delta_A) \cos(2\gamma_A - 2\psi) = -\sin^2 \delta_R \sin(4\gamma_R - 4\psi), \quad (31b)$$

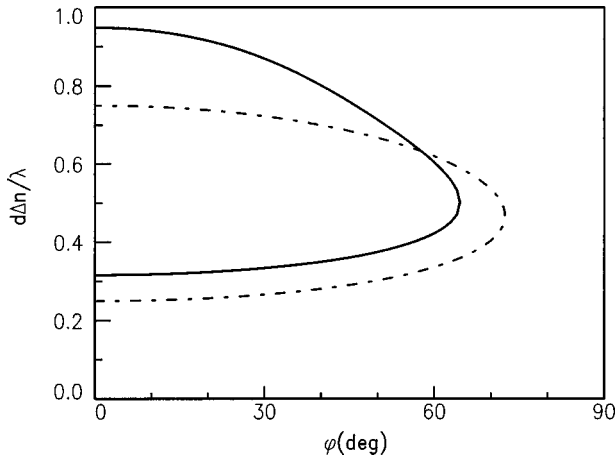


FIG. 9. The optimum ratio $d\Delta n/\lambda$ as a function of ϕ according to numerical calculations (full line) and according to the analytical approximation of Fig. 8 (dashed-dotted line).

$$\sin(\delta_A)\sin(2\gamma_A - 2\psi) = \cos^2 \delta_R + \sin^2 \delta_R \cos(4\gamma_R - 4\gamma), \quad (31c)$$

$$\cos(2\delta_B) = \cos \delta \cos(2\delta_R) + \sin \delta \sin(2\delta_R) \cos(2\gamma_R - 2\psi), \quad (31d)$$

$$\begin{aligned} \sin(2\delta_B) \cos(2\gamma_B - 2\psi) \\ = -\cos \delta \sin(2\delta_R) \cos(2\gamma_R - 2\psi) \\ + \sin \delta [\cos^2 \delta_R - \sin^2 \delta_R \cos(4\gamma_R - 4\psi)], \end{aligned} \quad (31e)$$

$$\begin{aligned} \sin(2\delta_B) \sin(2\gamma_B - 2\psi) = -\cos \delta \sin(2\delta_R) \sin(2\gamma_R - 2\psi) \\ - \sin \delta \sin^2 \delta_R \sin(4\gamma_R - 4\psi). \end{aligned} \quad (31f)$$

It turns out that only four of these six relations are independent, as the parameters on the left hand side of Eqs. (31) satisfy

$$\begin{aligned} \cos^2(2\delta_A) + \sin^2(\delta_A) \cos^2(2\gamma_A - 2\psi) \\ + \sin^2(2\delta_A) \sin^2(2\gamma_A - 2\psi) = 1, \end{aligned} \quad (32a)$$

$$\begin{aligned} \cos^2(2\delta_B) + \sin^2(2\delta_B) \cos^2(2\gamma_B - 2\psi) \\ + \sin^2(2\delta_B) \sin^2(2\gamma_B - 2\psi) = 1, \end{aligned} \quad (32b)$$

for all values of the parameters appearing on the right hand side of Eqs. (31). This is related to the unitarity of Jones matrices. Of the four remaining independent relations one is a relation between the liquid crystal parameters only. Namely, Eqs. (31) can be combined to

$$\cos(2\delta_A) \cos(2\delta_B) + \sin(2\delta_A) \sin(2\delta_B) \cos(2\gamma_A - 2\gamma_B) = 0, \quad (33)$$

a relation which does not involve the polarization or waveplate parameters. This requirement imposes a constraint on the parameters of the liquid crystal. More specifically, it gives the relation between the twist angle ϕ and the retardance to wavelength ratio $d\Delta n/\lambda$ as a function of the two driving voltages and the liquid crystal and cell parameters. It follows that this relation is independent of possibly present retarders and of the orientation of the liquid crystal with

respect to the incident and selected polarization. Figure 9 shows the numerically calculated relation between ϕ and $d\Delta n/\lambda$ for a liquid crystal layer with elastic constants $K_1 = 2K_2 = K_3 = 15$ pN, dielectric constants $\epsilon_\perp = 3.0$ and $\epsilon_\parallel = 8.0$, pretilt angle 2° , and driving voltages for state A and B equal to 1.0 and 5.0 V. The numerical result is qualitatively similar to the analytical approximation. The $d\Delta n/\lambda$ values are somewhat higher for the exact numerical result. The maximum twist angle is approximately 65° compared to 72° for the approximate analytical result. Finally, it is mentioned that there are other branches with higher ϕ and $d\Delta n/\lambda$ values than the plotted branch. These may be appropriate for passively driven displays, which require effects with a high twist angle.

Equation (33) is related to a theorem derived in the analysis of gray scale inversion in transmissive twisted nematic LCDs.¹⁹ According to this theorem the difference in reflection (or transmission) coefficient for voltages V_A and V_B is bound by a maximum, which does not depend on the incident or selected polarization, nor on the properties of possibly present retarders

$$|R_A - R_B| \leq \sin \tau. \quad (34)$$

The angle τ describing the maximum reflection difference can be expressed in terms of the Jones matrices for V_A and V_B by

$$\begin{aligned} \cos \tau = \frac{1}{2} \text{Tr}[\mathcal{J}_A \mathcal{J}_B^{-1}] = \cos(2\delta_A) \cos(2\delta_B) \\ + \sin(2\delta_A) \sin(2\delta_B) \cos(2\gamma_A - 2\gamma_B). \end{aligned} \quad (35)$$

Here, Tr indicates the trace of a matrix, which is defined as the sum of its diagonal elements. For optimum brightness and contrast one of the reflection coefficients must be equal to zero and the other equal to unity. This optimum can only be obtained when the angle τ is equal to $\pi/2$. It follows from Eq. (35) that this requirement is equivalent to Eq. (33).

When the liquid crystal parameters are such that Eq. (33) is satisfied there are three independent Eqs. (31) left that relate the polarization angle ψ , the waveplate retardation δ_R and optical axis angle γ_R and the effective retardation δ of state B. It follows that one of these four parameters can be chosen freely. This single free parameter can be used to optimize the LCD for a third favorable property (besides brightness and contrast), such as the color purity of the dark state. In the following δ_R is assumed to have a fixed value. The polarization angle ψ and the waveplate optical axis angle γ_R (and also the parameter δ) can then be solved in terms of the liquid crystal parameters and δ_R . It follows from Eq. (31a) that $\gamma_R - \psi$ satisfies

$$\sin(2\gamma_R - 2\psi) = \frac{\cos(2\delta_A)}{\sin(2\delta_R)}, \quad (36a)$$

$$\cos(2\gamma_R - 2\psi) = \frac{\sqrt{\sin^2(2\delta_R) - \cos^2(2\delta_A)}}{\sin(2\delta_R)}. \quad (36b)$$

Equations (31b) and (31c) can then be written as

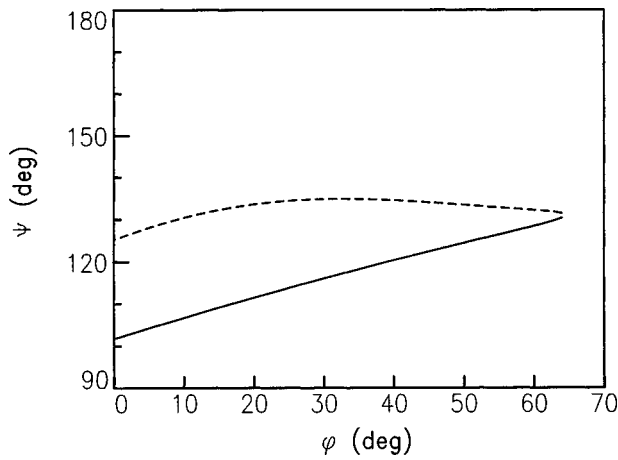


FIG. 10. The polarization angle ψ as a function of the liquid crystal twist angle ϕ for the liquid crystal parameters used in Fig. 9 and for $\delta_R = \pi/4$. The driven state is compensated such that the equivalent retarder is a $\lambda/2$ plate with optical axis at 45° with the polarizer. The full and dashed lines refer to the lowest and highest $d\Delta n/\lambda$ value of the full line in Fig. 9, respectively.

$$\sin(2\delta_A)\cos(2\gamma_A - 2\psi) = -\frac{\cos(2\delta_A)\sqrt{\sin^2(2\delta_R) - \cos^2(2\delta_A)}}{2\cos^2\delta_R}, \quad (37a)$$

$$\sin(2\delta_A)\sin(2\gamma_A - 2\psi) = \frac{2\cos^2\delta_R - \cos^2(2\delta_A)}{2\cos^2\delta_R}, \quad (37b)$$

leading to

$$\tan(2\gamma_A - 2\psi) = \frac{\cos^2(2\delta_A) - 2\cos^2\delta_R}{\cos(2\delta_A)\sqrt{\sin^2(2\delta_R) - \cos^2(2\delta_A)}}, \quad (38)$$

from which ψ can be solved easily. Using Eqs. (36) γ_R can then be found. With the aid of any one of the three remaining Eqs. (31d), (31e), and (31f), the parameter δ (the overall effective retardance of state B) may be found. According to Eqs. (36) δ_R and the difference between γ_R and ψ are restricted to the range

$$\frac{\pi}{4} - \delta_A \leq \delta_R \leq \frac{\pi}{4} + \delta_A, \quad (39a)$$

$$\frac{\pi}{4} - \delta_A \leq \gamma_R - \psi \leq \frac{\pi}{4} + \delta_A. \quad (39b)$$

In case state A is the driven state, δ_A is relatively small. This implies that δ_R and $\gamma_R - \psi$ are close to $\pi/4$, i.e., the retarder must be close to a $\lambda/4$ waveplate with an optical axis oriented at approximately 45° with the entry polarization. Figures 10 to 13 show numerically calculated values of ψ and γ_R for $\delta_R = \pi/4$ (the compensating waveplate is a $\lambda/4$ plate) and for the liquid crystal parameters of Fig. 9. State A is taken to be driven state of the liquid crystal in the calculation for Figs. 10 and 11. This corresponds to a normally white direct view display or to a normally black projection display. State B is taken to be the driven state of the liquid crystal in the calculation for Figs. 12 and 13. This corresponds to a

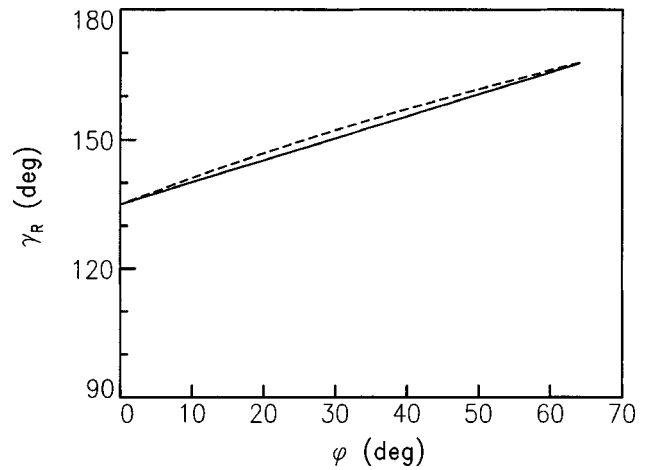


FIG. 11. The retarder optical axis orientation γ_R as a function of the liquid crystal twist angle ϕ for the parameter setting used in Fig. 10.

normally black direct view display or to a normally white projection display. Curves for other values of δ_R can be calculated in a similar way.

V. SUMMARY AND CONCLUSION

The Jones 2×2 matrix method is applied to reflective LCDs. Two general results established in the original Jones papers turn out to be of great use. According to the first result the Jones matrix for backward propagation is equal to the transpose of the Jones matrix for forward propagation. A consequence of this result is that the combined Jones matrix for reflection is a symmetric matrix. The second general result is that any Jones matrix can be represented by the product of the Jones matrices for a retarder and a rotator. Because of the symmetry of the reflection Jones matrix the rotation angle describing the effective rotator equals zero. It follows that a reflective LCD effectively behaves as a single retardation layer.

This equivalent retarder picture allows for a formulation of conditions for minimum and maximum reflection, i.e., conditions for high brightness and contrast. For a direct view display the polarizer is also the analyzer. Zero reflection is obtained if the equivalent retarder is a $\lambda/2$ plate with optical axis at 45° with the polarizer. Maximum reflection is obtained if the optical axis of the equivalent retarder is parallel or perpendicular to the polarizer and/or if the equivalent retarder has zero retardation. For a projection display the conditions for minimum and maximum reflection are the other way around, as now the selected polarization is perpendicular to the incident polarization.

These conditions can be applied to twisted nematics in order to optimize brightness and contrast. When the residual retardation of the driven state is neglected no compensating waveplate is needed. In this case analytical expressions for the twist angle and retardance to wavelength ratio may be derived. When the residual retardation of the driven state is taken into account numerical calculations are required to optimize the display performance. These calculations are greatly simplified by analytical results derived from the conditions on the equivalent retarder parameters. The first ex-

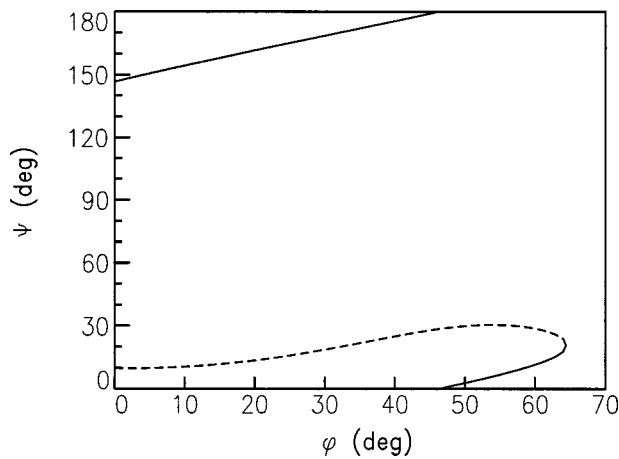


FIG. 12. The polarization angle ψ as a function of the liquid crystal twist angle ϕ for the liquid crystal parameters used in Fig. 9 and for $\delta_R = \pi/4$. The nondriven state is compensated such that the equivalent retarder is $\lambda/2$ plate with optical axis at 45° with the polarizer. The full and dashed lines refer to the lowest and highest $d\Delta n/\lambda$ value of the full line in Fig. 9, respectively.

presses the relation between the twist angle and the liquid crystal retardance to wavelength ratio. This relation does not depend on the nature of the compensating waveplate or on the entry polarization. The other results are expressions for the orientation of the compensator optical axis and of the entry polarization as a function of the retardation of the compensator and the liquid crystal parameters.

For the sake of simplicity only relatively small twist angles are considered. The results therefore apply to active matrix displays. Passive matrix displays use liquid crystal layers with a higher twist angle in order to obtain the required steep electro-optic response. A similar treatment as presented in this article is quite possible.

Another generalization of the presented results is to the Jones method for obliquely incident light.^{19,20,21} It turns out that the Jones matrix for reflection is then no longer equivalent to that of a single retardation layer. The methods for optimization outlined in this article are therefore not appropriate for obliquely incident waves.

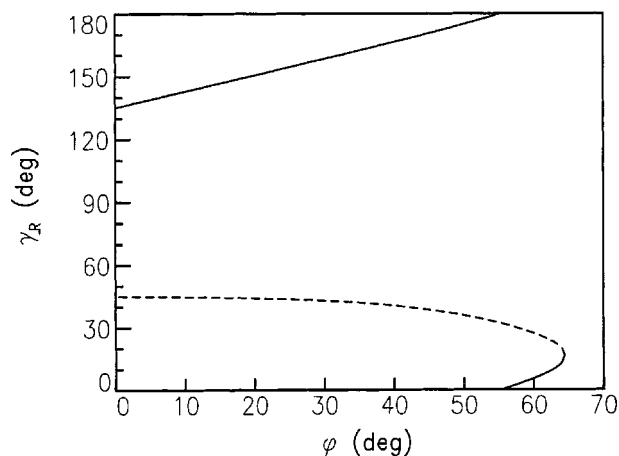


FIG. 13. The retarder optical axis orientation γ_R as a function of the liquid crystal twist angle ϕ for the parameter setting used in Fig. 12.

APPENDIX: RELATION WITH BERREMAN 4×4 MATRIX METHOD

The Maxwell equations for light propagating through a birefringent layer with normal along the z axis can be reduced to a set of four coupled first order equations for the x and y components of the electric and magnetic fields.^{22,1} For normal incidence these equations can be written as

$$\frac{d}{dz} \begin{bmatrix} E_x \\ \mu_0 c H_y \\ E_y \\ -\mu_0 c H_x \end{bmatrix} = ik \begin{bmatrix} 0 & 1 & 0 & 0 \\ P_{11} & 0 & P_{12} & 0 \\ 0 & 0 & 0 & 1 \\ P_{21} & 0 & P_{22} & 0 \end{bmatrix} \begin{bmatrix} E_x \\ \mu_0 c H_y \\ E_y \\ -\mu_0 c H_x \end{bmatrix}, \quad (\text{A1})$$

where c is the speed of light in vacuum, μ_0 the permeability of vacuum, where $k = 2\pi/\lambda$, with λ the vacuum wavelength, and where the coefficients P_{lm} depend on the components of the dielectric tensor according to

$$P_{11} = \epsilon_{xx} - \frac{\epsilon_{xz}\epsilon_{zx}}{\epsilon_{zz}}, \quad (\text{A2a})$$

$$P_{12} = \epsilon_{xy} - \frac{\epsilon_{xz}\epsilon_{zy}}{\epsilon_{zz}}, \quad (\text{A2b})$$

$$P_{21} = \epsilon_{yx} - \frac{\epsilon_{yz}\epsilon_{zx}}{\epsilon_{zz}}, \quad (\text{A2c})$$

$$P_{22} = \epsilon_{yy} - \frac{\epsilon_{yz}\epsilon_{zy}}{\epsilon_{zz}}. \quad (\text{A2d})$$

For a uniaxially birefringent medium with no optical activity the P_{lm} can be expressed in terms of the ordinary and extraordinary refractive index n_o and n_e , respectively, and the optical axis tilt and twist angles θ and ϕ , which are defined as the angle between the optical axis and the xy plane and the angle between the optical axis and the xz plane, respectively. The resulting expressions are

$$P_{11} = n_o^2 + \frac{n_o^2(n_e^2 - n_o^2)\cos^2\theta}{n_o^2\cos^2\theta + n_e^2\sin^2\theta} \cos^2\phi, \quad (\text{A3a})$$

$$P_{12} = P_{21} = \frac{n_o^2(n_e^2 - n_o^2)\cos^2\theta}{n_o^2\cos^2\theta + n_e^2\sin^2\theta} \sin\phi \cos\phi, \quad (\text{A3b})$$

$$P_{22} = n_o^2 + \frac{n_o^2(n_e^2 - n_o^2)\cos^2\theta}{n_o^2\cos^2\theta + n_e^2\sin^2\theta} \sin^2\phi. \quad (\text{A3c})$$

In the absence of absorption the refractive indices are real, implying that the coefficients P_{lm} are real as well.

Eliminating the magnetic field components of Eq. (A1) gives the following pair of second order differential equations for E_x and E_y

$$\frac{d^2}{dz^2} \begin{bmatrix} E_x \\ E_y \end{bmatrix} = -k^2 \begin{bmatrix} P_{11} & P_{12} \\ P_{21} & P_{22} \end{bmatrix} \begin{bmatrix} E_x \\ E_y \end{bmatrix}. \quad (\text{A4})$$

We look for first order equations of the form

$$\frac{d}{dz} \begin{bmatrix} E_x \\ E_y \end{bmatrix} = \pm ik \begin{bmatrix} N_{11} & N_{12} \\ N_{21} & N_{22} \end{bmatrix} \begin{bmatrix} E_x \\ E_y \end{bmatrix}, \quad (\text{A5})$$

that are equivalent to Eq. (A4). The set of equations with the positive sign refer to the wave propagating in the $+z$ (forward) direction, whereas the set of equations with the negative sign refer to the wave propagating in the $-z$ (backward) direction. Clearly, the backwardly propagating solution can be obtained from the forwardly propagating solution by simply replacing the term ik by $-ik$. The refractive indices are real when there is no absorption. It turns out that then the N_{lm} are real as well. The substitution $ik \rightarrow -ik$ is then equivalent to taking the complex conjugate.

The first order Eq. (A5) give rise to the second order equations

$$\frac{d^2}{dz^2} \begin{bmatrix} E_x \\ E_y \end{bmatrix} = -k^2 \begin{bmatrix} N_{11}^2 + N_{12}N_{21} & N_{12}N_{11} + N_{21}N_{22} \\ N_{21}N_{11} + N_{12}N_{22} & N_{22}^2 + N_{12}N_{21} \end{bmatrix} \begin{bmatrix} E_x \\ E_y \end{bmatrix} \pm ik \frac{d}{dz} \begin{bmatrix} N_{11} & N_{12} \\ N_{21} & N_{22} \end{bmatrix} \begin{bmatrix} E_x \\ E_y \end{bmatrix}. \quad (\text{A6})$$

The second term on the right-hand side may be neglected provided that the coefficients N_{lm} vary little over one wavelength

$$\frac{1}{\lambda} \left| \frac{dN_{lm}}{dz} \right| \ll 1. \quad (\text{A7})$$

The second term even vanishes when the N_{lm} are constant. In these cases the first order Eq. (A5) are equivalent to the Maxwell equations if

$$P_{11} = N_{11}^2 + N_{12}N_{21}, \quad (\text{A8a})$$

$$P_{12} = N_{12}N_{11} + N_{21}N_{22}, \quad (\text{A8b})$$

$$P_{21} = N_{21}N_{11} + N_{12}N_{22}, \quad (\text{A8c})$$

$$P_{22} = N_{22}^2 + N_{12}N_{21}. \quad (\text{A8d})$$

The coefficients N_{lm} can now be solved using Eq. (A3)

$$N_{11} = n_o + \Delta N \cos^2 \phi, \quad (\text{A9a})$$

$$N_{22} = n_o + \Delta N \sin^2 \phi, \quad (\text{A9b})$$

$$N_{12} = N_{21} = \Delta N \sin \phi \cos \phi, \quad (\text{A9c})$$

with the effective birefringence

$$\Delta N = \frac{n_o n_e}{\sqrt{n_o^2 \cos^2 \theta + n_e^2 \sin^2 \theta}} - n_o. \quad (\text{A10})$$

For a tilt angle θ equal to zero we find $\Delta N = \Delta n \equiv n_e - n_o$, i.e., the effective birefringence is equal to the real birefringence. If Δn is sufficiently small the effective birefringence ΔN is equal to $\Delta n \cos^2 \theta$.

The solution of Eq. (A5) for forward propagation can be written as

$$\begin{bmatrix} E_x \\ E_y \end{bmatrix}_{\text{out}} = \mathcal{J} \begin{bmatrix} E_x \\ E_y \end{bmatrix}_{\text{in}}. \quad (\text{A11})$$

The explicit expression for the Jones matrix \mathcal{J} in this particular case is

$$\mathcal{J} = \exp(i\alpha) \mathcal{R}(\phi) \mathcal{U}(\delta) \mathcal{R}(-\phi). \quad (\text{A12})$$

The phase difference between the two eigenwaves is

$$2\delta = \frac{2\pi d \Delta N}{\lambda}, \quad (\text{A13})$$

and the overall phase α , which can usually be left out, is given by

$$\alpha = \frac{2\pi d(n_o + \Delta N/2)}{\lambda}. \quad (\text{A14})$$

It turns out that the Jones matrix of this single uniform layer is symmetric, i.e., it is equal to its transpose

$$\mathcal{J} = \mathcal{J}^T. \quad (\text{A15})$$

The solution of Eq. (A5) for backward propagation

$$\begin{bmatrix} E'_x \\ E'_y \end{bmatrix}_{\text{in}} = \mathcal{J}' \begin{bmatrix} E'_x \\ E'_y \end{bmatrix}_{\text{out}}, \quad (\text{A16})$$

follows from Eq. (A11) by replacing ik , i.e., by $-ik$, i.e., by replacing δ by $-\delta$ and α by $-\alpha$. An additional matrix inversion is needed because the field at $z=0$ is now expressed in terms of the field at $z=d$ instead of the other way around. Matrix inversion also boils down to replacing δ by $-\delta$ and α by $-\alpha$. It follows that combining the substitution $ik \rightarrow -ik$ with matrix inversion leaves the Jones matrix unchanged. Consequently, the Jones matrix for backward propagation is equal to the Jones matrix for forward propagation

$$\mathcal{J}' = \mathcal{J}. \quad (\text{A17})$$

Combining this equation with Eq. (A15) it is found that

$$\mathcal{J}' = \mathcal{J}^T. \quad (\text{A18})$$

Now consider a stack of M different birefringent layers. The gist of the 2×2 Jones matrix approach is the neglect of all reflection effects at the interfaces between the different layers. This implies that forward and backward propagation remain decoupled throughout the whole stack. As a consequence, the overall Jones matrix for forward propagation can be expressed in terms of the individual Jones matrices for forward propagation $\mathcal{J}_1, \dots, \mathcal{J}_M$ as

$$\mathcal{J} = \mathcal{J}_M \dots \mathcal{J}_2 \mathcal{J}_1. \quad (\text{A19})$$

The overall Jones matrix for backward propagation is then

$$\mathcal{J}' = \mathcal{J}'_1 \mathcal{J}'_2 \dots \mathcal{J}'_M = \mathcal{J}_1^T \mathcal{J}_2^T \dots \mathcal{J}_M^T = \mathcal{J}^T. \quad (\text{A20})$$

Clearly, relation (A18) also holds for a stack of different but uniform birefringent layers. On the other hand, relation (A17) no longer holds for such a stack. Relation (A18) also holds for nonuniform birefringent layers, provided that the N matrix varies slowly over a wavelength. In that case the Jones method can be correctly applied. The nonuniform layer is then approximated by a stack of different but uniform sublayers, for which Eq. (A18) is satisfied. For a large number of sublayers the approximation becomes exact, implying that Eq. (A18) holds for both nonuniform and uniform layers.

A more direct proof is possible when there is no absorption present. Then the Jones matrix for backward propagation for an arbitrary stack of layers is found by complex conjugation combined with matrix inversion

$$\mathcal{J}' = \mathcal{J}^{*-1}. \quad (\text{A21})$$

If the birefringent layers are nonabsorbing the Jones matrix \mathcal{J} is a unitary matrix, meaning that

$$\mathcal{J}^{-1} = \mathcal{J}^\dagger, \quad (\text{A22})$$

where the dagger indicates the combined operation of transposition and complex conjugation. It then follows that \mathcal{J}' is related to \mathcal{J} by Eq. (A18).

¹S. Stallinga, J. Appl. Phys. **85**, 3023 (1999).

²R. C. Jones, J. Opt. Soc. Am. **31**, 488 (1941).

³N. Vansteenkiste, P. Vignolo, and A. Aspect, J. Opt. Soc. Am. A **10**, 2240 (1993).

⁴H. Hurwitz, Jr. and R. C. Jones, J. Opt. Soc. Am. **31**, 493 (1941).

⁵R. C. Jones, J. Opt. Soc. Am. **31**, 500 (1941).

⁶K. Lu and B. E. A. Saleh, Appl. Opt. **30**, 2354 (1991).

⁷T. J. Scheffer and J. Nehring, Seminar Notes, Society for Information Display, Orlando, FL, May 23–25 1995.

⁸T. Sonehara, Jpn. J. Appl. Phys., Part 2 **29**, L1231 (1990).

⁹H. S. Kwok, J. Appl. Phys. **80**, 3687 (1996).

¹⁰S. T. Wu and C. S. Wu, Appl. Phys. Lett. **68**, 1455 (1996).

¹¹E. Beynon, K. Saynor, M. Tillin, and M. Towler, Symposium Digest, Society for Information Display, Boston, MA, May 11–16 1997, p. L34.

¹²H. A. van Sprang, US Patent No. 5,490,003 (28 June 1991).

¹³K. H. Yang and M. Lu, IBM J. Res. Dev. **42**, 401 (1998).

¹⁴M. D. Tillin, M. J. Towler, K. A. Saynor, and E. J. Beynon, Symposium Digest, Society for Information Display, Anaheim, CA, May 17–22 1998, p. 311.

¹⁵E. Sakai, H. Nakamura, K. Yoshida, and Y. Ugai, Proceedings of the International Display Workshop, Kobe, November 27–29 1996, p. 329.

¹⁶S. T. Tang, F. H. Yu, J. Chen, M. Wong, H. C. Huang, and H. S. Kwok, J. Appl. Phys. **81**, 5924 (1997).

¹⁷S. T. Wu and C. S. Wu, Liq. Cryst. **24**, 811 (1998).

¹⁸S. T. Wu and C. S. Wu, J. Appl. Phys. **83**, 4096 (1998).

¹⁹S. Stallinga, J. M. A. van den Eerenbeemd, and J. A. M. M. van Haaren, Jpn. J. Appl. Phys., Part 1 **37**, 560 (1998).

²⁰P. Yeh, J. Opt. Soc. Am. **72**, 507 (1982).

²¹C. Gu and P. Yeh, J. Opt. Soc. Am. **10**, 966 (1993).

²²D. W. Berreman, J. Opt. Soc. Am. **62**, 502 (1972).